EFDA–JET–CP(09)06/58

S. Jachmich, T. Eich, G. Arnoux, W. Fundamenski
and JET EFDA contributors

Comparison of Power Peposition Profiles During ELMs using Langmuir Probes and Infra-Red Camera Diagnostic at JET

Comparison of Power Peposition Profiles During ELMs using Langmuir Probes and Infra-Red Camera Diagnostic at JET

S. Jachmich[1], T. Eich[2], G. Arnoux[3], W. Fundamenski[3]
and JET EFDA contributors*

JET-EFDA, Culham Science Centre, OX14 3DB, Abingdon, UK

[1]Association EURATOM-Belgian State, Koninklijke Militaire School - Ecole Royale Militaire, B-1000 Brussels Belgium
[2]Max-Planck Institut fuer Plasmaphysik, Euratom Association, Garching, Germany
[3]EURATOM-UKAEA Fusion Association, Culham Science Centre, OX14 3DB, Abingdon, OXON, UK
** See annex of F. Romanelli et al, "Overview of JET Results", (Proc. 22 nd IAEA Fusion Energy Conference, Geneva, Switzerland (2008)).*

Preprint of Paper to be submitted for publication in Proceedings of the
36th EPS Conference on Plasma Physics, Sofia, Bulgaria.
(29th June 2009 - 3rd July 2009)

1. INTRODUCTION

Characterising the energy SOL transport during Type I ELMs in JET is of major interest to understand the empirical scaling of ELM heat fluxes to the ITER. The separation of the transient pulses of heat and particles arriving at the divertor target plates as a consequence of upstream ELM activity delivers insight of the convective and conductive transport channels. Such efforts require measurement of the ELM behaviour with both high temporal and spatial resolution, which can be achieved by infrared- and Langmuir probe measurements.

2. DIAGNOSTIC SET-UP

In the MkIIHD-divertor an array of twelve Langmuir Probes (LP) had been installed in between the toroidal gaps. At each seven poloidal positions on the outer-strike plate the divertor is equipped with three probes, which can be operated as triple probe at a time resolution of 100μs (see Fig.1). The probes, which are at the same poloidal location, are toroidally separated by about 0.7m to avoid any possible flux tube cross-talk. Further five probes can be operated as single probe (with a poloidal spatial resolution of about 1.5cm), which provide more accurate analysis by applying probe voltage sweeping with 170Hz, which is, hence, restricted to inter-ELM phases. When operated as triple probe the electron temperature is estimated from the voltage difference between an electron collecting and a floating pin:

$$T_e = (V_r - V_{fl}) / \ln (1 + A_{is}/A_r) \qquad (1)$$

Since the divertor probes at JET are wedge shaped, the pins suffer from erosion over time. Regular calibration pulses are used to cross-calibrate the areas. Implying an uncertainty in the effective probe areas of 10%, results in errors of the electron temperature measurement of about 25%. This error could be significantly reduced by increasing the ratio of the probe areas. In two identical, consecutive pulses the two methods, single and triple probe technique has been compared. Fig.2 shows the radial profile of the electron temperature during a strike point sweep on the Load Bearing Septum Replacement Plate (LBSRP) – the outer divertor target plate. Within the measurement uncertainty good agreement of both techniques has been found. The heat flux is inferred from the measured particle flux and electron temperature assuming a constant sheath transmission factor of 8.

The surface temperature of the outer target is measured by an infrared camera (FLIR ATS system) with high spatial (2mm on the LBSRP) and time (up to 35μs) resolution. In this paper, the time resolution of the IR data is 86μs (corresponding to a sampling rate of ~11kHz), and the target heat fluxes are calculated using the non-linear code THEODOR [1]. Note that a thin uniform carbon layer [2, 3] is assumed for the heat load calculation, with a heat transmission factor $\sigma = 200$kW/mK.

3. POWER DEPOSITION PROFILES

The LP- and IR-data have been taken during steady state phases of low triangularity ($\delta \approx 0.24$) ELMy H-mode discharges with plasma current scan from 1.5 to 2.5MA, q_{95}-scan from 3.4 to 5.6, neutral beam power scan from 5 to 15MW and deuterium gas scan up to 1.9 10^{22} el/sec. The typical

ELM size achieved in these plasmas ranges from 50 to 250kJ corresponding to an ELM energy drop of 5% of the plasma energy. The ELMs were coherently averaged typically over two seconds during each flat top phase of the discharge. For each ELM a standard deviation from the averaged ELM has been defined as $\int_1^2 (P(t)-\langle P\rangle(t))^2 dt/(t_2-t_1)$. ELMs lying outside of a 3σ–window were excluded from the average.

Figures 3 and 4 show radial profiles of the heat fluxes mapped to the outer midplane in between ELMs and at the time of the ELM-peak power respectively with a constant q95 of 5.6 and pedestal collisionality ν^*_{ped} of 0.4 (blue), 0.3 (red) and 0.2 (green). Positive radial values correspond to the scrape-off layer, negative to the private-flux region. The strike point position is inferred from the magnetic equilibrium code EFIT [4]. Typically the outer strike point is about 3-5cm further in than determined by EFIT. Good quantitative agreement of both diagnostics has been found. Compared to LPs, the larger heat flux in the private flux region measured by the IR has two origins: 1) The IR measurement includes the heat due to plasma radiation, and 2) an additional background caused by reflection of IR emission from the wall onto the divertor is measured, which are of course not detected by the LPs, since they are sensitive only to particle flux.

As can be inferred from the figures the radial decay lengths increase drastically during the ELMs. One should note the double exponential shape of the inter-ELM profiles, which has also been reported earlier [5, 6]. The IR-power fluxes at the ELM-peak exhibit a bump in the profile. This is most likely due to the assumption of a radially, uniform correction for the CFC layer [5, 6]. Radial decay lengths have been determined taking into account data larger than 1/e of the maximum. The results are summarized in figures 5 and 6. As expected the decay length increases strongly with the edge safety factor due to longer connection length. From a least square fit the following scalings have been revealed:

$$\text{inter-ELM: } \lambda_r \propto q_{95}^{1.6}\, \nu^{*-0.015}_{ped}, \qquad \text{ELM-peak: } \lambda_r \propto q_{95}^{2.5}\, \nu^{*\,0.13}_{ped}$$

In a similar fashion the ELM-duration has been characterized by calculating a typical decay time after the ELM-peak. For low as well as high q_{95}, the data suggest longer decay times for higher edge pedestal collisionality. Due to the longer connection length from the midplane to the divertor target at higher q_{95}, ions diffuse more into the SOL before reaching the target, leading to longer radial decay length and shorter ELM-duration. This is supported by the empirical scaling $\lambda_r \propto q_{95}^{-2.8}\, \nu^{*\,0.88}_{ped}$ as shown in figure 7.

CONCLUSIONS

Good agreement of IR- and LP-measured power fluxes assuming a constant sheath transmission factor γ during ELMs has been found. A possible enhancement of γ during the ELM lies within the measurement uncertainty. The magnetic connection length has twofolded effect on the ELM-transport. On one hand, longer connection length lead to further broadening of the deposition profile, on the other hand concomitantly shortens the ELMduration.

ACKNOWLEDGEMENT

This work, supported by the European Communities under the contract of Association between EURATOM and Belgian State, was carried out within the framework of the European Fusion development Agreement. The views and opinions expressed herein do not necessarily reflect those of the European Commission.

REFERENCES

[1]. A. Herrmann *et al*., Plasma Physics Controlled Fusion **37** (1995), p. 17.
[2]. P. Andrew *et al*., Journal Nuclar Materials **337-339** (2005), p. 146.
[3]. T. Eich et al., Plasma Physics Controlled Fusion **49** (2007), p. 573.
[4]. D. P. O'Brien *et al*., Nuclear Fusion **32** (1992), p. 1351.
[3]. V. Riccardo *et al*., Plasma Physics Controlled Fusion **43** (2001), p. 881.
[4]. W. Fundamenski *et al*., Nuclear Fusion **45** (2005), p. 950.

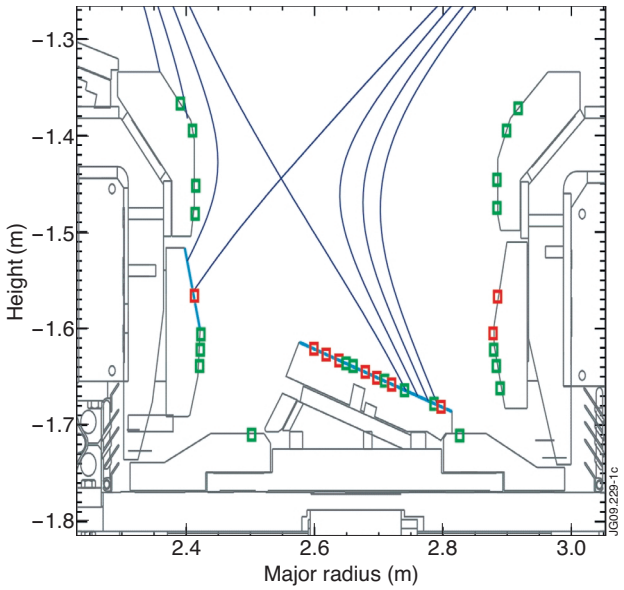

Figure 1: Cross-section through divertor indicating positions of triple (red squares) and single probes (green squares). The flux surfaces shown are 3mm apart at the outer midplane.

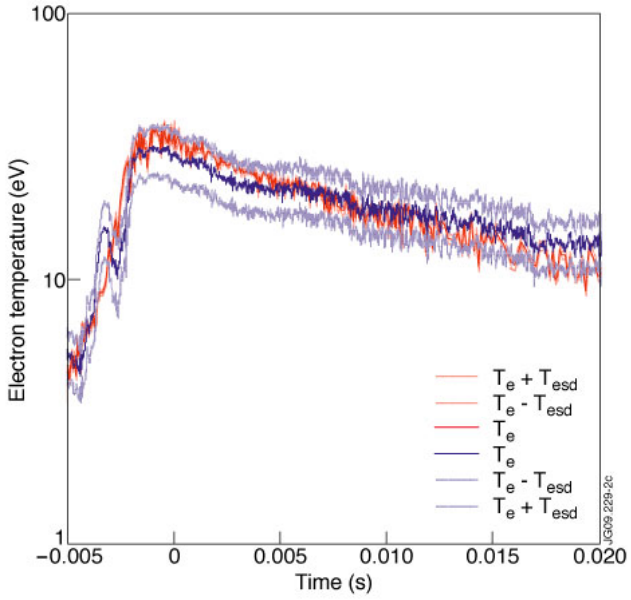

Figure 2: Electron temperature profile measured by single and triple probe. Light colours indicate errorbars of the data.

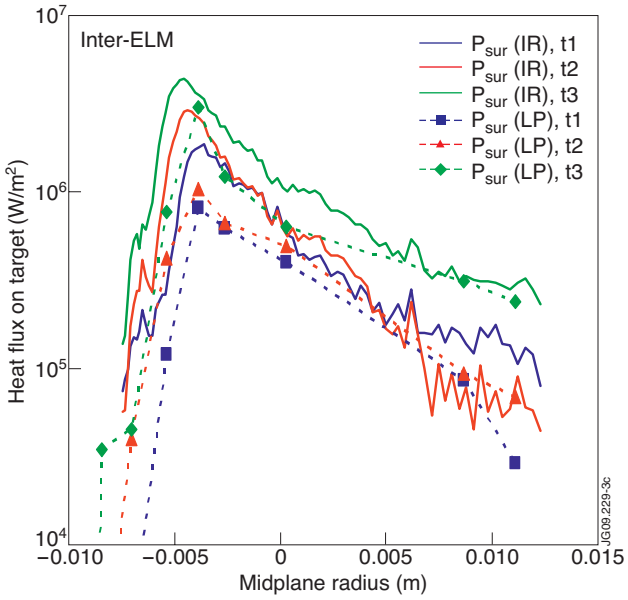

Figure 3: Heat flux profiles measured by IR and LP in between ELMs at $q_{95} = 5.6$ and ν^*_{ped} from 0.2 to 0.4.

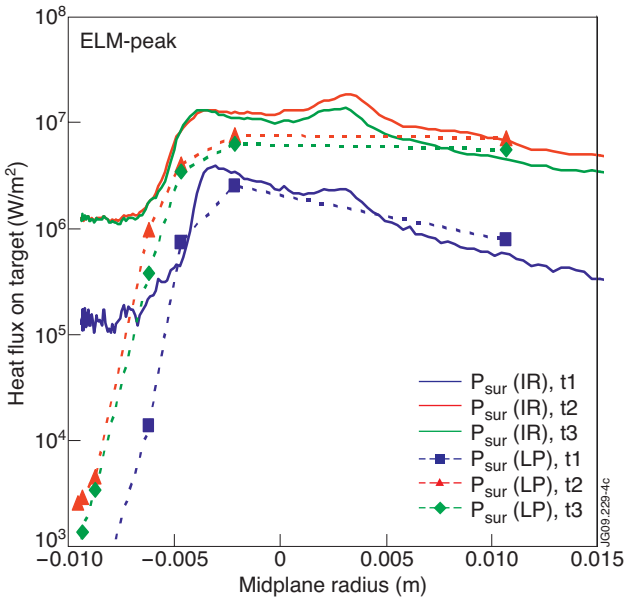

Figure 4: Heat flux profiles measured by IR and LP at the time of the ELM-peak at $q_{95} = 5.6$ and ν^*_{ped} from 0.2 to 0.4.

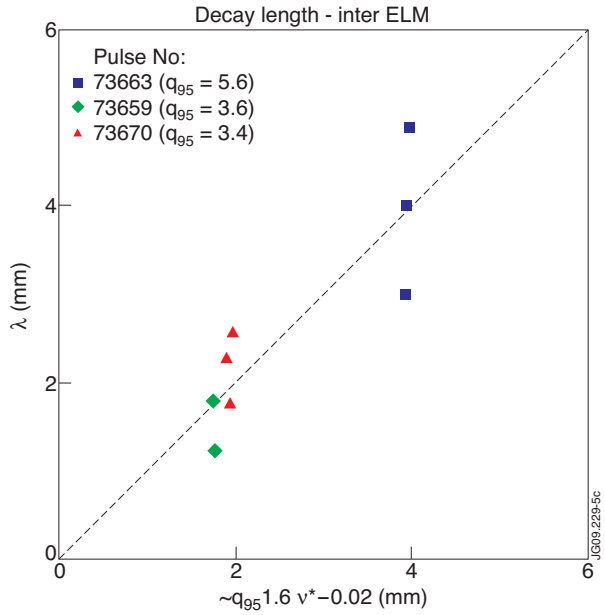

Figure 5: Decay length of inter-ELM heat flux profiles.

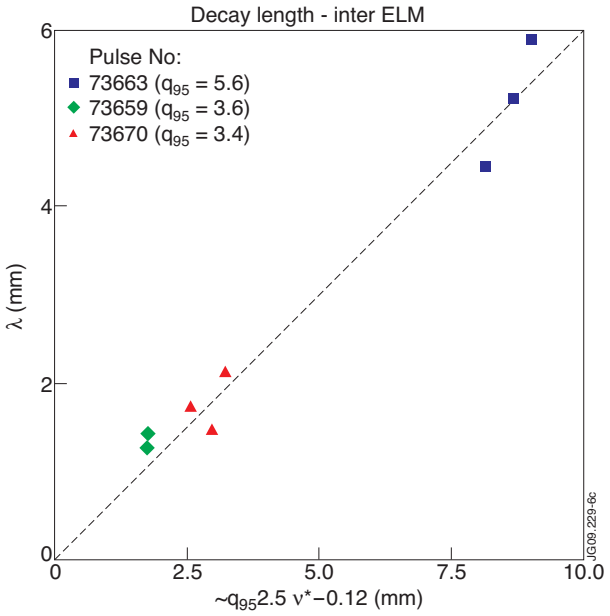

Figure 6: Decay length of heat flux profiles at the time of the ELM-peak.

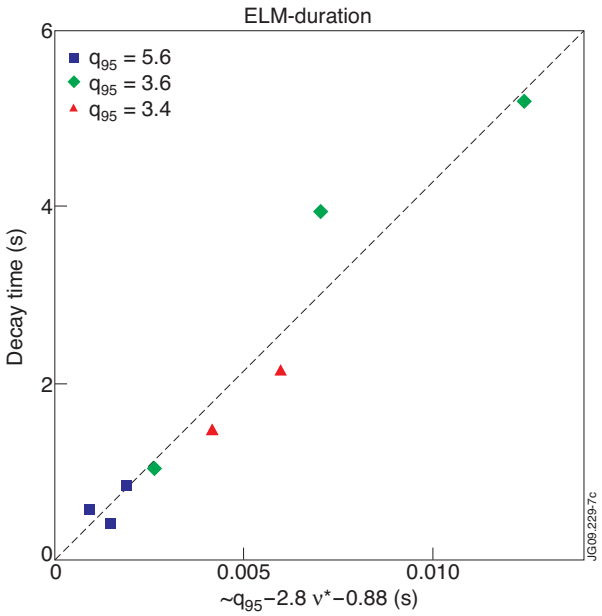

Figure 7: Decay times of heat flux measured at the strike-zone.